PROCEEDINGS OF SCIENCE

CVD-Diamond Detectors – R&D Status and New Results

First Author1 **E. Berdermann**
Affiliation *GSI Helmholtz Zentrum für Schwerionenforschung*
Address, Country *Planckstrasse 1, 64291 Darmstadt, Germany*
E-mail: e.berdermann@gsi.de

Another Author **W. de Boer**
Affiliation *Karlsruhe Institute of Technology (KIT)*
Address, Country *Kaiserstrasse 12, 76131 Karlsruhe, Germany*
E-mail: deboer@ekp.physik.uni-karlsruhe.de

Another Author **M. Ciobanu**
Affiliation *GSI Helmholtz Zentrum für Schwerionenforschung*
Address, Country *Planckstrasse 1, 64291 Darmstadt, Germany*
E-mail: m.ciobanu@gsi.de

Another Author **S. Dunst**
Affiliation *University of Augsburg*
Address, Country *Universitätsstrasse 1, 86159 Augsburg, Germany*
E-mail: stefan.rudolf.dunst@student.uni-augsburg.de

Another Author **M. Kiš**
Affiliation *GSI Helmholtz Zentrum für Schwerionenforschung*
Address, Country *Planckstrasse 1, 64291 Darmstadt, Germany*
E-mail: m.kis@gsi.de

Another Author **W. Koenig**
Affiliation *GSI Helmholtz Zentrum für Schwerionenforschung*
Address, Country *Planckstrasse 1, 64291 Darmstadt, Germany*
E-mail: w.koenig@gsi.de

Another Author **P. Moritz**
Affiliation *GSI Helmholtz Zentrum für Schwerionenforschung*
Address, Country *Planckstrasse 1,64291 Darmstadt, Germany*
E-mail: p.moritz@gsi.de

Another Author **J. Morse**
Affiliation *European Synchrotron Radiation Facility (ESRF)*
Address, Country *Rue Jules Horowitz 6, 38043 Grenoble, France*
E-mail: morse@esrf.fr

[1] Speaker: E. Berdermann

PoS(BORMIO2010)040

PROCEEDINGS OF SCIENCE

Another Author **S. Müller**
Affiliation *Karlsruhe Institute of Technology (KIT)*
Address, Country *Kaiserstrasse 12, 76131 Karlsruhe, Germany*
E-mail: steffen.mueller@cern.ch

Another Author **C. Nociforo**
Affiliation *GSI Helmholtz Zentrum für Schwerionenforschung*
Address, Country *Planckstrasse 1, 64291 Darmstadt, Germany*
E-mail: c.nociforo@gsi.de

Another Author **M. Pomorski**
Affiliation *CEA-LIST Saclay*
Address, Country *91191 Gif-sur-Yvette, France*
E-mail: michal.pomorski@cea.fr

Another Author **M. Schreck**
Affiliation *University of Augsburg*
Address, Country *Universitätsstrasse 1, 86159 Augsburg, Germany*
E-mail: Matthias.Schreck@Physik.Uni-Augsburg.de

Another Author **M. S. Rahman**
Affiliation *GSI Helmholtz Zentrum für Schwerionenforschung*
Address, Country *Planckstrasse 1, 64291 Darmstadt, Germany*
E-mail: M.S.Rahman@gsi.de

Another Author **M. Träger**
Affiliation *GSI Helmholtz Zentrum für Schwerionenforschung*
Address, Country *Planckstrasse 1, 64291 Darmstadt, Germany*
E-mail: m.traeger@gsi.de

Another Author **H. Weick**
Affiliation *GSI Helmholtz Zentrum für Schwerionenforschung*
Address, Country *Planckstrasse 1, 64291 Darmstadt, Germany*
E-mail: h.weick@gsi.de

We report on the status of diamond detectors developed for atomic, nuclear, and hadron physics experiments at GSI, the Helmholtz Center for Heavy Ion Research and at FAIR, the upcoming Facility for Antiproton and Ion Research, both situated in Darmstadt, Germany. Three types of intrinsic diamond materials produced by Chemical Vapour Deposition (CVD) on various substrates have been evaluated for time- and energy measurements: (a) homoepitaxial single-crystal CVD Diamond (scCVDD) grown on High Pressure High Temperature (HPHT) single-crystal diamond plates, (b) polycrystalline CVD Diamond (pcCVDD) grown on silicon wafers, and (c) CVD Diamond on Iridium (DoI) samples, consisting of 'quasi-single-crystal' CVD diamond films grown on iridium substrates. We discuss the detector characteristics of each type and describe the perspectives for the diamond detectors in current and future experiments.

XLVIII International Winter Meeting on Nuclear Physics - BORMIO2010
Bormio, Italy
January 25–29 2010

PoS(BORMIO2010)040

1. Introduction

The main advantages of wide band gap detector materials such as diamond (E_g^{Dia} = $5.48eV^{T=300K}$) are their radiation hardness and room temperature detector operation without the need of a pn-junction and cooling to control leakage current. Diamond is unique in its combination of extreme electronic and thermal properties. It reveals equally high drift velocities of electrons and holes at electric fields E ≥ 10 V/μm ($v_{e,h}$ = 1.43 x 10^7 cm/s [1]), a low dielectric constant (ε_r = 5.7), and exceptionally high breakdown fields $E_B \geq 10^7$ V/cm. Thermal gradients in diamond are restricted due to its thermal conductivity 20 $Wcm^{-1}K^{-1}$, which is six times higher than the one of copper. Nitrogen (N) and boron (B) impurities are immanent trace elements in most natural diamonds and are the origin of inferior material parameters. We investigated therefore only intrinsic pc- and scCVDD samples supplied by DDL [2], which have nominal concentrations N < 5ppb (scCVDD) to N ≤ 50 ppb (pcCVDD) and boron B < 1 ppb (scCVDD) to B < 5 ppb (pcCVDD), respectively. The 'early' DoI samples discussed in this report are grown with high-purity hydrogen and methane at the University of Augsburg.

The pcCVDD samples consist typically of large-grain columnar diamond crystals which are separated by large-angle grain boundaries. Due to the growth conditions, in most cases the films have a (110) fibre texture. The grain boundaries represent structural defects that reveal a high concentration of charge-trapping centers. The Charge Collection Efficiency (CCE) of pcCVDD detectors used 'As Grown' (AG) is rather low (CCE ≈ 10% to 25%). Thinning from the nucleation side, i.e. the side closest to the substrate during the growth, provides a more homogeneous diamond film of large grain size and a CCE up to 60%: this material is denominated 'Detector Grade' (DG) pcCVDD. In contrast, growth on HPHT diamond substrates with carefully prepared, smooth surfaces provides mono-crystalline sensors with negligible dislocations and with a CCE ≈ 100%. On the other hand, the small size (max-area ≈ $1cm^2$) of scCVDD is a limitation for many applications. A promising route towards large-area 'quasi-single-crystal' devices was the invention of heteroepitaxy on Iridium (d_{Ir} = 3.834Å). Using e-beam evaporation at temperatures T > 700^0C, iridium films of about 100nm thickness are produced on wafer-scale multilayer structures [3].

In this article, we discuss the status of the detector investigations and the potential of diamond sensors for central applications in 'hadron physics' research.

2. Characteristics of Diamond Detectors

2.1 Original diamond signals (pcCVDD, scCVDD, DoI)

The performance of diamond detectors for timing and spectroscopy is tested with the Transient Current Technique (TCT) using ^{241}Am-α-particles of a very short range of R_{Dia} ≈ 12μm [4][5]. Depending on the polarity of the applied high voltage (HV) bias, either electrons or holes drift only a short distance d_{drift} < 12μm and contribute very little to the induced current I_{ind}. Figure 1 shows Transient Current (TC) signals in detectors fabricated with the various diamond materials discussed above. Hole-drift signals are plotted on the left-hand graph and electron-drift pulses on the right-hand graph, respectively. The signals have been read out from

the HV side electrode(s) with Diamond Broadband Amplifiers (DBA [5]) and recorded with a 3GHz Digital Storage Oscilloscope (DSO) with 20Gsamples/s. The pulse shape $I_{ind}(t_{drift}) \propto E_{int}(d_{drift})$ reveals the internal field profile [6] and the corresponding single-carrier drift properties.

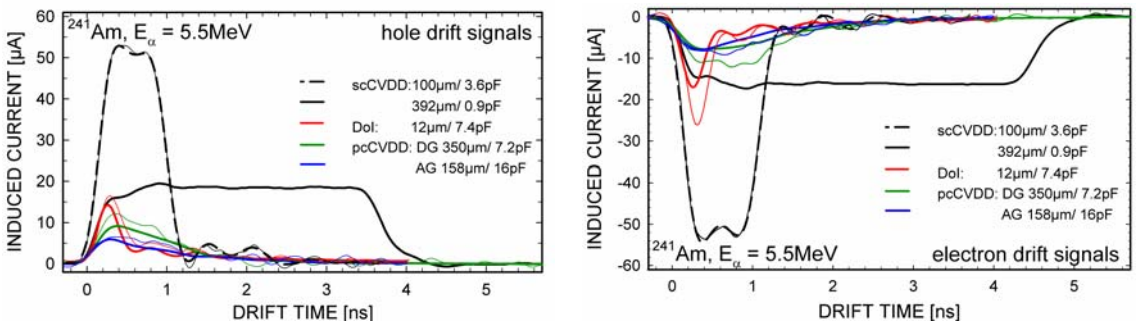

Figure 1. ^{241}Am-α-signals in CVDD sensors of different quality and thickness measured with the same external field E_{ext} = ± 3V/µm. The pulse shapes depict the internal field profile $E_{int}(d_{drift})$ of each sensor type indicated by the line colors (thin lines: single-pulses, thick lines: averaged).

The trapezoidal shape of the scCVDD signals demonstrates the case of an ideal detector of parallel-plate geometry for which the internal field E_{int} is constant and equal to the externally applied field E_{ext}. The α-induced charge drifts to the opposite electrode and the sample thickness dependent signal width (Fig. 1, thick black dashed and solid lines) corresponds to the single-carrier drift path (FWHM $\Rightarrow d_{drift} = d_D$). The signal area $\int I(t)\cdot dt \,|\, \Delta t_{drift}$ is proportional to the measured charge. Excellent energy resolution is expected if single and average pulses are identical. Deviations from the trapezoidal shape indicate charge losses (CCE << 100%) and such sensors (pcCVDD and DoI) cannot be used for spectroscopy. The early DoI samples discussed in this article revealed more trapping than expected but showed relatively high amplitudes of less dispersion than those of pcCVDD detectors (sect. 2.3). We measured similar rise times of $t_{rise} \approx 230$ ps, all limited by the bandwidths of the DBA and DSO electronics. The signal width of low-quality sensors is defined by the lifetime of the charge carriers ($d_{drift} << d_D$) and by the detector capacitance C_D. Accordingly, the rate capability of scCVDD counters is 10^8 to 10^7 ions/s for samples of 50 to 500 µm thickness, respectively, and up to 10^9 ions/s for pcCVDD and DoI detectors with optimized low capacitances.

2.2 Heavy-ion beam diagnostics and ToF detectors (pcCVDD, scCVDD, DoI)

All three diamond detector types are capable of high-rate counting (sect. 2.1). Detection efficiency close to 100% is achieved by selecting the CCE and the sample thickness according to the specific energy loss dE/dx of the particles of interest, taking into account the pair-production energy of diamond, $\varepsilon_{Dia} = 12.84$ eV [1]. Diamond beam monitors are unique in the sense that a single detector is capable of measuring in single-particle counting mode particle rates varying from a single ion to 10^9 ions/s, and much higher rates in current-integrated mode. We have developed beam diagnostic devices (pcCVDD) for high-frequency accelerator bunch

and spill analysis as well as beam- and beam-loss monitors for slow and fast extracted ions [7]. For intense, highly focused and bunched beams (as used for instance at GSI in Plasma Physics experiments) homogeneous detectors (scCVDD) have been provided [8].

Diamond start detectors for heavy-ion ToF systems should have an intrinsic time resolution σ_i superior to the resolution of the standard ToF detectors by least a factor of two. σ_i is proportional to the noise dispersion, σ_{noise}, and inversely proportional to the slope of the leading edge dV_{Dia}/dt of the signal. It is therefore not evident a priori that scCVDD sensors will in all cases be preferable start detectors. Intrinsic time resolutions of $\sigma_i \approx 29$ ps and $\sigma_i \approx 110$ ps have been achieved for ^{52}Cr ions (Z = 24) of 650 AMeV and for relativistic ^{12}C ions (Z = 6) of 2.0 AGeV, respectively (HADES [9]) using 100μm thick AG pcCVDD sensors with DBA signal readout. Measurements performed with relativistic ^{27}Al ions of 2.0 AGeV using pc- and scCVDD sensors and a four-channel amplifier-discriminator card FEE-1 showed a near identical time resolution of $\sigma_i \leq 28$ps (FOPI [10]), confirming that σ_i is in practice limited by the noise and the bandwidth of present state of the art electronics.

2.3 Start detectors for relativistic light ions and protons (scCVDD)

Relativistic particles of Z = 1 slowing down in diamond generate a signal charge of 36e per micrometer. Into a 50Ω load, this gives 29μV for protons and 260μV for ^{6}Li ions, assuming sensors of 300μm thickness and CCE ≈ 1. In comparison, the DBA noise voltage to consider for a good resolution is $3\sigma_{noise} \approx 135\mu$V. Due to the poor S/N ratios, pcCVDD sensors may show low detection efficiency in such cases. Extended simulations and tests predict best results for low-capacitance, broadband amplifiers of low $C_i << 1$pF, and assemblies with minimized detector (C_D) and parasitic capacitances (C_P). In October 2009, the time resolution of scCVDD quadrant sensors was tested with ^{6}Li ions of E = 1.8AGeV using both modular (FEE-1 (mod.), $d_D = 400\mu$m) and integrated (LCBBA-1, $d_D = 100\mu$m) detector assemblies. FEE-1 (mod.) was read out via capacitive buffers followed by FEE-1 cards modified for analogue processing (MOS-follower; 1MΩ, 2.1pF, 1GHz). The diamond sensors of the integrated assembly LCBBA-1 were mounted on the FEE boards and wire bonded to active impedance transformers of C_i = 0.2 pF. The signals were subsequently shaped with fast booster amplifiers. The quadrant-detector sector capacitances were low in both cases ($C_{D\text{-}400}$ = 0.2 pF and $C_{D\text{-}100}$ = 0.9 pF) compared to the parasitic capacitance values C_P = 4pF for FEE-1 (mod.) and C_P = 1.7pF for LCBBA-1 measured, respectively. The time-difference spectra obtained with these assemblies are shown in Figure 2 (blue and red curves) together with a proton spectrum (green lines) measured with an older LCBBA amplifier design (LCBBA-0; $d_D = 300\mu$m, $C_D \approx 0.3$pF, $C_P \approx$ 2.5pF) which achieved σ_i = 101ps [11]. For clarity, an offset has been added to each Y-data set. The histograms show the experimental data and the smooth lines are the corresponding Gaussian fits.

Preliminary resolutions of σ_{DT} = 77 ps and σ_i = 55 ps have been obtained for the FEE-1 (mod.) assembly by selecting prompt time coincident events with high signal amplitudes. The LCBBA-1 data are walk-corrected and processed under the condition that no neighbor sectors have triggered. Using a new amplifier transistor (SiGe:C; BFR705L3RH) an excellent σ_i = 32ps was achieved, of which the diamond contribution was 21ps. Previous estimations [10] supported

by these results predict that a detector thickness d_D = 100µm is adequate for many experiments with swift heavy and light particles, despite the larger C_D and the lower induced signal charge

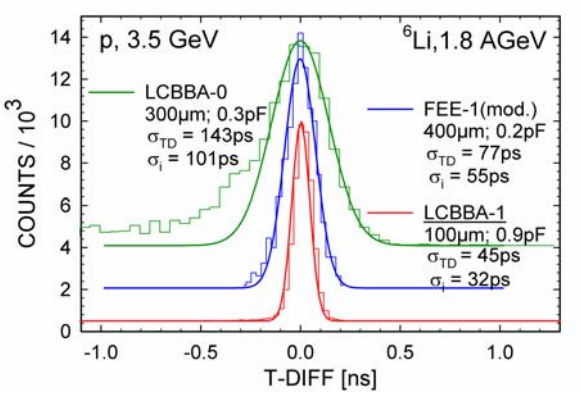

Figure 2. Improved time resolution of scCVDD sensors for relativistic protons and light ions achieved with low-capacitance assemblies. A σ_i = 101 ps was measured for protons in 2007 (LCBBA-0, green lines), and in October 2009, σ_i = 32ps (LCBBA-1, red lines) and σ_i = 55ps (FEE-1 mod., blue lines) for ^{6}Li ions of 1.8AGeV. (see text)

obtained compared to measurements performed with thicker samples. The reason is the dominance of the higher slope dV/dt of the TCT signals of thin sensors (Fig. 1). Superior resolution will in the future be possible with fast-ASIC readout [12].

2.4 Detectors for beam-energy- and ion-spectroscopy measurements (scCVDD)

Only homogeneous sensors showing trapezoidal TC-α-signals (CCE ≈ 1) are applicable for energy-loss spectroscopy (sect. 2.1). The energy resolutions of homo and heteroepitaxial CVDD samples are compared by their 'broadband line widths' δE_x where we find δE_{Dia}/ δE_{DoI} / $\delta E_{DG\text{-}PC}$ ≈ 1/ 2/ 4 (Fig. 3, Left).

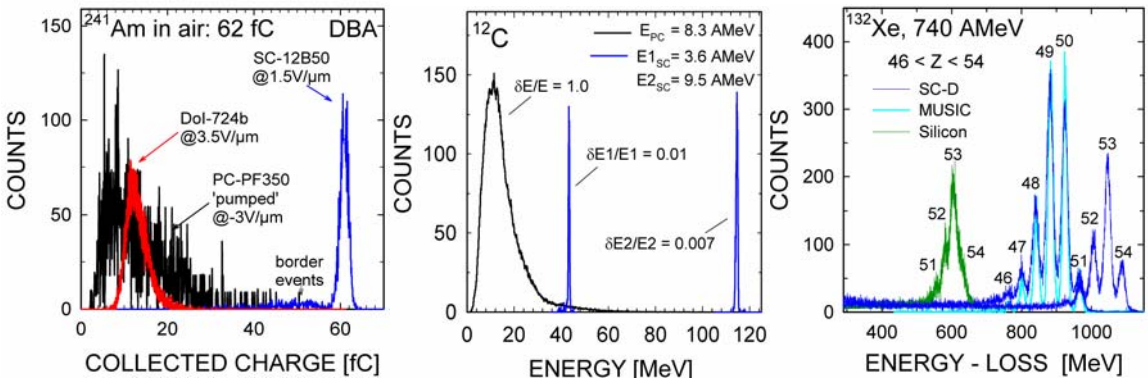

Figure 3. (Left) α-spectra measured with sc (blue)-, pc (black)-, and DoI (red) CVDD detectors using DBAs. (Center) Low-energy ^{12}C distributions of pc (black) and scCVDD (blue) sensors. (Right) Relativistic heavy-ion spectra obtained with scCVDD (blue), silicon (green), and gaseous ionization chambers (cyan) using high-resolution spectroscopy electronics.

These results are also confirmed as high-resolution energy measurements performed with commercial spectroscopy electronics developed for silicon detectors (Figs. 3, central and right part, respectively). The peak value of the ^{12}C spectrum measured with a pcCVDD detector (black line) is ≈ 85% lower than the expected value of 99.6 MeV. In contrast, both lines measured with a scCVDD sensor correspond exactly to the energy of the ^{12}C ions. Moreover,

while the relative resolution of the polycrystalline sensor is $\delta E_{Dia}/\Delta E_{Dia} = 1.0$, the corresponding resolution of the scCVDD sensor (blue lines) reaches values ≤ 0.01, which are similar to those obtained with silicon detectors working under the same conditions (i.e. without cooling). For energy losses of the order of 1 GeV, as it is the case of ^{131}Xe fragments, the performance of scCVDD (right plot, blue lines) was found far superior to silicon (green) and its particle-identification capability approaching that of MUSIC chambers (cyan). These data have been obtained in a fragmentation experiment at the FRS of GSI with the test detectors mounted in air. In contrast to the silicon detectors, diamond sensors do not show pulse-height defects and (similar to MUSICs) they are insensitive for high energetic δ-electrons influencing the energy-loss straggling and thus the energy resolution. More details can be found in [13][14].

3. A radiation hardness study with scCVDD samples

We irradiated scCVDD samples with protons of $E_p = 26$ MeV and neutrons of $E_n = 20$ MeV up to fluencies of $\Phi \approx 10^{16}$ p,n/cm^2 [1][15]. Subsequently measured optical absorption spectroscopy data revealed neutral vacancies (V^0) as the main radiation-induced defect. Similar defect production rates $\beta_{e,h}$ were found for both p- and n irradiation. The parameter $\beta_{e,h} \approx 10^{-15}$ cm²/ns is calculated according to the relation $1/\tau_{eff} = \beta \cdot \Phi$ (Fig. 4, Left) after accounting for the effective trapping time τ_{eff} extracted from TC signals (Fig. 4, right). τ_{eff} and CCE $\propto v_{e,h} \cdot \tau_{eff}$ both decreases in proportion to Φ.

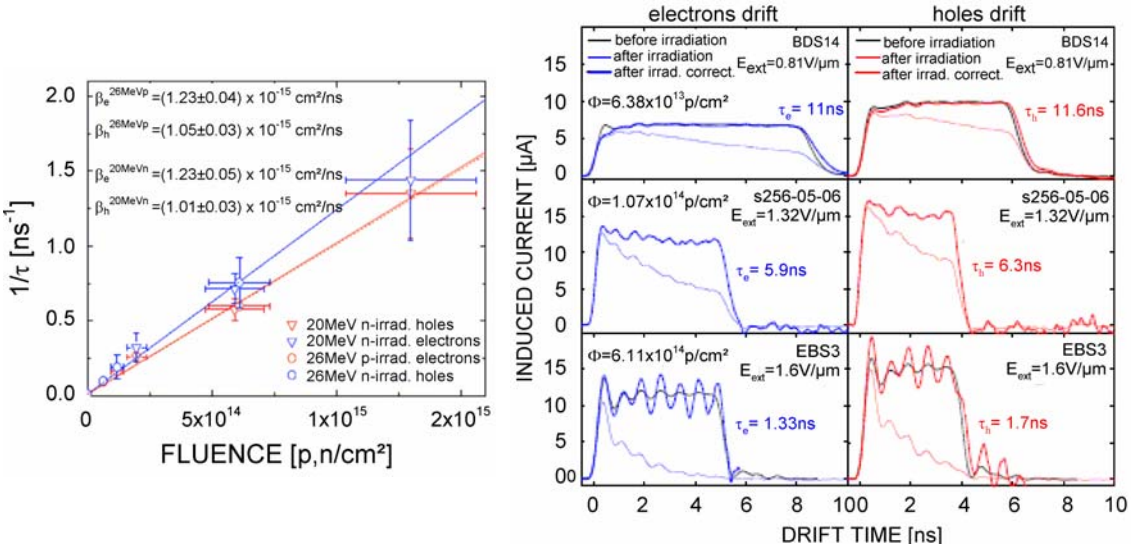

Figure 4. (Left) Defect production rates ($\beta_{e,h}$) of scCVDD after irradiation with 26 MeV protons and 20 MeV neutrons: electron data are plotted in blue and hole data in red. (Right) TCT α-signals of samples BDS14, s256-05-06, and EBS-3 in the virgin state (trapezoidal shapes) and after irradiation with protons (slopes on flat top, thin lines) up to fluencies Φ, respectively. After trapping correction the signals (thick lines) reproduce those of the virgin detectors.

Signal rise times and amplitudes were preserved even after fluencies of $\Phi = 6x10^{14}$ p/cm², and thus, the time resolution as well. The width of signals obtained after irradiation was

unchanged, confirming that (for unprimed detectors) the internal field is unchanged and that the radiation induced defects are mainly neutral vacancies (V^0). In a real experiment, a slightly different E_{int} may occur due to the charging of the V^0 centers by the electrons or holes trapped. However, we expect similar velocities also in that case, since the defect density is low even after high-dose irradiation. Although the charge loss is significant (reduced signal area), the corresponding spectroscopy signals of high-energy ^{90}Sr-β-particles (i.e. MIP) showed a mean value of 2000e, and were clearly separated from the electronic noise. In conclusion, the timing properties of proton detectors were almost unchanged up to fluencies of $\Phi \approx 10^{15}$ p/cm^2, whereas after exposure to still higher fluencies no TC-α-pulses have been obtained. The collected charge was decreased by a factor of three after irradiations of a $\Phi \approx 10^{16}$ p/cm^2 [1].

4. Status of Technology

4.1 Detector bulk materials (scCVDD, DoI)

Isolated threading dislocations are frequently observed in scCVDD samples that lead to reduced HV stability of the fabricated sensors, which otherwise show excellent charge-collection and timing properties at low fields [1][10][16]. They originate from dislocations already present in the bulk of the HPHT substrates or from dislocations generated by the surface polishing of the HPHT crystals propagating into the overgrown CVDD film. Nucleation on iridium substrates yields a unique nucleation density and alignment of diamond grains. The material starts with a very high density of dislocations. With increasing thickness the grains merge, and the mosaic spread as well as the dislocation density decreases forming a defective single crystal.

4.2 Detector electrodes (scCVDD)

The objective is to produce electrodes on inert, high-resistivity diamond with an oxygen terminated surface, which prevents electron injection from the metal into the diamond. This permits the application of large bias voltage, enabling effective and rapid access of particle-induced charge from the crystal [3]. Accumulation of charge carriers under such a 'blocking contact' alters the internal field profile, which becomes strongest at that contact and reduced towards the opposite electrode. At high particle-rate operation, charge accumulation may take place and the electrodes will start 'leaking' up to the complete detector break down. So far we have obtained the best results from scCVDD samples of perfectly reconstructed and polished surfaces with rms roughness < 1nm. CVDD detectors can be metallized using standard photolithography techniques with micro-patterned electrodes for position-sensitive readout.

Conclusions and Outlook

The most versatile type of artificial diamond is the scCVDD, which has a CCE ≈ 100% together with the highest drift velocities for electrons and holes. Samples made with high-quality contacts can be operated at electric fields as high as 10 V/μm and are capable of usually contradictory applications: (a) fast counting and timing with an intrinsic resolution of $\sigma_i << 50$ps and (b) energy measurements with a precision which is comparable to gaseous ionization

chambers. scCVDD sensors can be used for beam diagnostics, for ToF and spectroscopy of ions and protons as well as for the vertex detection in high-energy experiments.

pcCVDD and DoI samples make large-area diamond detectors possible, preferably for timing, counting, and tracking applications for which a reduced CCE is acceptable. The higher spatial homogeneity of the DoI sensors, in addition to extremely narrow signal shape of relatively high amplitudes, open perspectives for improved large-area tracking and ToF devices that are capable of operating at the highest ion rates. Our attention is now focused on the growth and post processing as well as on the characterization of diamond plates grown on iridium. In addition, we are pursuing the fabrication and the test of low-capacitance single-channel amplifiers and of a broadband ASIC (PADI-4 [12]), which has been modified for single-MIP sensitivity and the readout of diamond strip sensors.

Acknowledgments

This work is supported by the EC through the Integrated Infrastructure Initiatives *HadronPhysics* (FP6, Proj. RII3-CT-2004-506078) and *HadronPhysics2* (FP7, Proj. RII3-CT_227431), and the Marie Curie project MC-PAD. We would like to thank the GSI members of the Target Laboratory for the diamond metallizations, the accelerator operating crew for the excellent beams, and in particular, Christophor Kozhuharov for his constant interest and many fruitful discussions.

References

[1] M. Pomorski, *PhD Thesis*, University of Frankfurt, 2008.

[2] Diamond Detector Ltd. (DDL), Dorset, UK (Distributer); Element Six, Ascot, UK, (Producer)

[3] S. Gsell, T. Bauer, J. Goldfuß, M. Schreck, B. Stritzker: *A route to diamond wafers by epitaxial deposition on silicon via iridium/yttria stabilized zirconia buffer layers*, Appl.Phys.Lett. **84** (2004) 4541

[4] E. Berdermann and M. Ciobanu, in: R. S. Sussmann (Edt.), CVD Diamond for Electronic Devices and Sensors, Wiley Series Materials for Electronic & Optoelectronic Applications (2009) 227

[5] P. Moritz, E. Berdermann, K. Blasche, H. Stelzer, B. Voss: *Broadband electronics for CVD-diamond detectors*, Diam. Relat. Mater. **10** (2001) 1770

[6] J. Isberg, A. Lindblom, A. Tajani, D. Twitchen, *Temperature dependence of hole drift mobility in high-purity single-crystal CVD diamond*, phys. stat. sol. (a) **202**, No. 11 (2005) 2194

[7] E. Berdermann, K. Blasche, H. W. Daues, P. Moritz, H. Stelzer, B. Voss, *The Diamond Project at GSI - Perspectives*, Proc. ICATPP-7, Como, Italy, (2001) 246

[8] J. Bol, E. Berdermann, W. de Boer, E. Grigoriev, F. Hauler, L. Jungermann, *Beam monitors for* TESLA based on diamond strip detectors, IEEE Transactions on Nuclear Science, 3, (2004) 1566

[9] The HADES Collaboration, *The high-acceptance dielectron spectrometer HADES,* EPJA **41** (2009) 243

[10] E. Berdermann, M. Pomorski, W. de Boer, M. Ciobanu, S. Dunst, C. Grah, M. Kiš, W. Koenig, W. Lange, W. Lohmann, R. Lovrinčić, P. Moritz, J. Morse, S. Mueller, A. Pucci, M. Schreck, MD. S.

Rahman, M. Traeger: *Diamond detectors for hadron physics research*, Diam. Relat. Mater. **19** (2010) 358

[11] J. Pietraszko, L. Fabbietti, W. Koenig, M. Weber, *Diamonds as timing detectors for minimum-ionizing particles: The HADES proton-beam monitor and START signal detectors for time of flight measurements*, NIM A **618** (2010) 121.

[12] E. Berdermann, M. Ciobanu, N. Herrmann, K. D. Hildenbrand, M. Kiš, W. Koenig, M. Pomorski, A. Schuettauf, *Diamond Start Detectors*, Proc. IEEE NSS-MIC, Orlando, 2009, Conference Record.

[13] E. Berdermann, M. Pomorski, A. Pullia, S. Riboldi, M. Traeger, H. Weick, D. Boutin, H. Geissel, Y. Litvinov, C. Nociforo, K. Suemmerer, M. Winkler, *Performance of Diamond Detectors in a Fragmentation Experiment*, Proc. XLV Int. Winter Meeting on Nuclear Physics, I. Iori (Ed.) (2007)

[14] E. Berdermann, A. Caragheorgheopol, M. Ciobanu, M. Pomorski, A. Pullia, S. Riboldi, M. Traeger, H. Weick, *Ion spectroscopy – a diamond characterization tool*, Diam. Relat. Mater. **17** (2008) 1159

[15] W. de Boer, J. Bol, A. Furgeri, S. Müller, C. Sander, E. Berdermann, M. Pomorski, M. Huhtinen, *Radiation hardness of diamond and silicon sensors compared*, phys. stat. sol. (a) 204, (2007) 3004

[16] J. Morse, M. Salomé, E. Berdermann, M. Pomorski, J. Grant, V. O'Shea, P. Ilinski, *Single-crystal CVD-diamond detectors: Position and temporal response measurements using a synchrotron microbeam probe*, Mater. Res. Soc. Symp., Proc. Fall 2007, Vol. 1039-P06-02